Friction **11**(6): 1094–1106 (2023)
https://doi.org/10.1007/s40544-022-0655-0
ISSN 2223-7690
CN 10-1237/TH
RESEARCH ARTICLE

A preliminary experimental investigation on the biotribocorrosion of a metal-on-polyethylene hip prosthesis in a hip simulator

Shu YANG[1,2], Jian PU[1], Xiaogang ZHANG[1,*], Yali ZHANG[1], Wen CUI[1], Fengbao XIE[2], Weiping LU[1], Qin TAN[1], Zhongmin JIN[1,3]

[1] *Tribology Research Institute, School of Mechanical Engineering, Southwest Jiaotong University, Chengdu 610031, China*

[2] *Beijing Chunlizhengda Medical Instruments Co., Ltd., Beijing 101100, China*

[3] *School of Mechanical Engineering, University of Leeds, Leeds LS2 9JT, UK*

Received: 07 November 2021 / Revised: 17 April 2022 / Accepted: 23 May 2022

Abstract: Corrosion at the taper/trunnion interface of total hip replacement (THR) often results in severe complications. However, the underlying mechanisms of biotribocorrosion at the taper/trunnion interface during the long-term walking gait cycles remain to be fully understood. In this study, a hip joint simulator was therefore instrumented with an electrochemical cell for *in-situ* monitoring of the tribocorrosion evolution in a metal-on-polyethylene (MoP) THR during a typical long-term walking gait. In addition, the biotribocorrosion mechanism was investigated via surface and chemical characterizations. The experimental results confirmed that the taper/trunnion interface dominated the contemporary MoP hip joint corrosion. Three cyclic variations in the open circuit potential (OCP) were observed throughout the long-term electrochemical measurements, attributed to the formation and disruption of the adsorbed protein layer. The corrosion exhibited an initial increase at each period, peaking at approximately 0.125 million cycles, followed by a subsequent gradual reduction. Surface and chemical analyses revealed the formation of a tribochemical reaction layer (tribolayer) on the worn surface of the taper/trunnion interface. The surface/chemical characterizations and the electrochemical measurements indicated that the adhesion force of the adsorbed protein layer was weaker than that of the tribolayer. In contrast, the opposite was true for the corrosion resistance. Based on the observations from this study, the tribocorrosion mechanism of the taper/trunnion interface under the long-term walking gait cycles is deduced.

Keywords: biotribocorrosion; metal-on-polyethylene (MoP); adsorbed protein layer; total hip replacement (THR)

1 Introduction

Charnley's metal-on-polyethylene (MoP) total hip replacement (THR) is widely regarded as the gold standard for end-stage arthritis treatment. Further improvements include modular designs, consisting of (taper/trunnion) interface, which is convenient for surgeons when treating a wide range of patients [1]. However, due to the cyclic loading, fretting-corrosion at the taper/trunnion may result in adverse local tissue reactions (ALTRs) [2], leading to pseudotumours and THR failure. An increasing number of ALTRs in MoP THRs has recently been reported. For example, the prevalence of revision surgery caused by ALTRs in MoP THRs is 0.5% and 3.2% at a mean follow-up of 7 years [3] and over 10 years [4], respectively. Due to the excellent clinical results of contemporary hip implants using highly cross-linked polymer (PE) or vitamin E diffused cross-linked PE, it seems that the wear problem of THR has been overcome. However, the fretting-corrosion at the taper/trunnion interface is still an engineering issue that has not been

* Corresponding author: Xiaogang ZHANG, E-mail: xg@swjtu.edu.cn

Nomenclature

MoP	Metal-on-polyethylene	LPR	Linear polarization resistance
THR	Total hip replacement	R_P	Polarization resistance
ALTRs	Adverse local tissue reactions	I_{corr}	Corrosion current
PE	Polymer	β_a, β_c	Tafel constants
MoM	Metal-on-metal	LSCM	Laser scanning confocal microscopy
UHMWPE	Ultra-high molecular weight polyethylene	SEM	Scanning electron microscopy
		R_Z	Surface roughness
EDTA	Ethylene diamine tetraacetic acid	EDS	Energy-dispersive X-ray spectroscopy
WE	Working electrode	TEM	Transmission electron microscopy
PEEK	Polyether ether ketone	AFM	Atomic force microscopy
OCP	Open circuit potential		

properly solved. As a result, much research focuses on understanding the fretting-corrosion at the taper/trunnion interface, including the visual inspection of fretting-corrosion damage from retrieved implants [5, 6], electrochemical assessment of material combination corrosion behavior in pin/ball-on-disc tests [7–9], and volume loss measurements of the hip joint taper/trunnion interface [10].

Retrieved implant analysis provides helpful information on the corrosion behavior under real circumstances. However, the limited number of samples and difficulty in changing the implant parameters result in challenges in identifying the evolution and mechanism of corrosion by this method. Combining a pin/ball-on-disc tribometer with an electrochemical cell is widely employed in research on the corrosion mechanisms of material combinations. However, the contact geometry, motion, and loading conditions at the modular junctions of THRs are distinct from those of simple tribometers. Thus, this method is unable to reflect the *in-vivo* environment. Simulator testing is the closest approach to clinical practice compared with other *in-vitro* test methods. Implementing a coordinate measuring machine allows directly determining the volume loss at the hip joint taper/trunnion interface from the hip joint simulator. Thus, volume loss measurements can evaluate the fretting-corrosion damage at the taper/trunnion junction more quantitatively than other assessments. Owing to the protection of the taper/trunnion interface from assembly and disassembly, the volumetric wear was measured prior to and after testing. Consequently, the volume loss measurements cannot trace the tribocorrosion evolution at the taper/trunnion junction during the test.

The tribocorrosion of metal-on-metal (MoM) THR has been well studied in an instrumented hip simulator [11–14]. However, to the best of the authors' knowledge, there is a lack of research that employs hip simulator tests to investigate the long-term biotribocorrosion at the MoP THR modular junctions. Therefore, this paper aims to investigate the long-term biotribocorrosion behavior of the MoP hip implant via an instrumented hip joint simulator and to attempt to explain the biotribocorrosion mechanism from the experimental observations.

2 Materials and methods

2.1 Test materials and specimens

Four sets of 28-mm diameter MoP hip prostheses were tested in this study. The taper/trunnion interface comprised a CoCrMo head (12/14 taper; ISO 5832-12) and a Ti–6Al–4V (TC4) stem (12/14 taper; ISO 5832-3). The stem and spigot (Fig. 1) were employed to represent the clinical femoral stem as they use the same morse taper design. The femoral heads and stems were assembled in a torsional testing machine

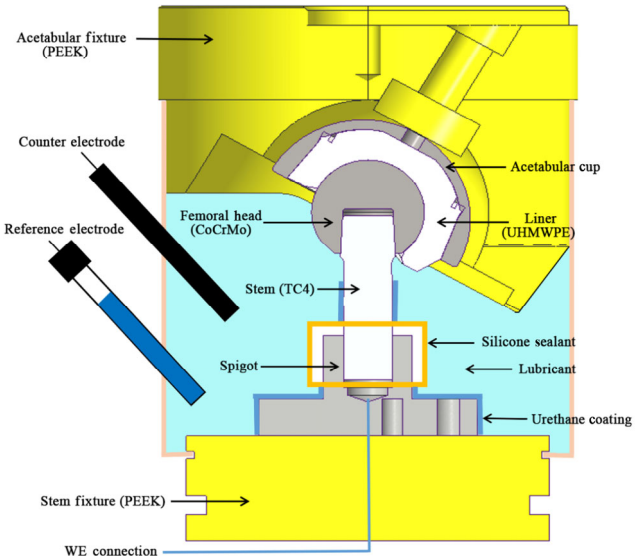

Fig. 1 Experimental setup demonstrating the working electrode (WE) connection to the stem and electrodes contained within the lubricant. Any possible metallic tribocorrosion sources were sealed via silicone sealant and urethane coating.

(E10000, Instron, USA) with a 2-kN axial force at a stroke rate of 0.04 mm/s (ISO 7206-10). The ultra-high molecular weight polyethylene (UHMWPE) liner was integrated with the femoral head to form the MoP articulations. All the test samples were provided by Beijing Chunlizhengda Medical Instruments Co., Ltd., China. The lubricant calf serum solution was prepared following the recommendation of ISO 14242-1 and Ref. [15]. Briefly, it was diluted to a total protein content of 30 g/L with deionized water and supplemented with ethylene diamine tetraacetic acid (EDTA), gentamicin, and amphotericin B to retard the precipitation of calcium phosphate and bacterial growth.

2.2 Experimental setup

The test samples were mounted on a 6-station hip joint simulator (Prosim, Simulation Solutions, UK) under a cup inclination angle of 60°. All the test specimens were subject to time-varying twin-peak load and relative articulating motion per ISO 14242-1 standard. The *in-situ* measurements of the MoP hip joint electrochemical reactions adopted a hip simulator with three-electrode electrochemical cells [11]. Figure 1 presents the schematic diagram of the experimental setup. The working electrode (WE) connection was placed at the stem bottom, and Ag/AgCl reference and platinum counter-electrodes were inserted into the container connecting the test cell. All possible sources of metallic tribocorrosion were sealed with silicone sealant and urethane coating. At the same time, sample mountings of polyether ether ketone (PEEK) were used to prevent any contributions to the electrochemical measurements. Sometimes, the machine stops due to the breakage of the silicon rubber case or the overvoltage of the power supply. The test samples were not removed from the simulator when dealing with the stop of the machine.

2.2.1 *Biotribocorrosion of MoP THR during long-term walking gait cycles*

The first test consisted of two sets of MoP THRs, which was conducted with the same test configuration to improve the reliability of the tests. These tests were referred to as Samples 1 and 2, and they were run for 1.5 million cycles at 1 Hz under the typical walking gait cycle. The *in-situ* corrosive degradation was monitored throughout the tests. Following ISO 14242-1, the fluid test medium was replaced every 0.5 million cycles. At each serum changing point, the serum was drained from the test cell and flushed three times with deionized water before refilling with fresh serum [16]. To minimize disturbances to the tribochemical reaction and protein adsorption layers at the taper/trunnion interface, the test samples were in place in the simulator when replacing the calf serum.

2.2.2 *Biotribocorrosion of the MoP THR bearing surface*

In the experimental setup (Fig. 1), the WE represented the entire exposed surfaces of the taper/trunnion interface and the head/liner articulation. Therefore, an additional series of tests was introduced to examine the articulation effects on the electrochemical measurements. The tests were based on several considerations. Firstly, to the best of the authors' knowledge, there are no reports of MoP THR clinical failure caused by corrosion from MoP bearing surfaces. Furthermore, Hesketh et al. [8] determined a 30-fold reduction in the MoP corrosion current (I_{corr}) compared to MoM material combinations. Hence, this study assumed that the taper/trunnion interface

(metal–metal contact) was the major source of metal ion release and MoP THR tribocorrosion. To further confirm this, the surface characterization of the femoral head bearing surface was examined before and after testing. Moreover, the clear cyclic variation of the open circuit potential (OCP) trends was observed at each serum changing point of the long-term tests. Thus, a test that ran for 0.5 million cycles (a typical serum changing point) was considered long enough to demonstrate the entire corrosion cyclic variation and distinguish the articulation effect on corrosion for the entire system. Last, since the movement during testing prevented the full sealing of the MoP articulation, the taper/trunnion interface was sealed with silicone sealant instead. This excluded any electrochemical measurements of the taper/trunnion interface, ensuring that only signals from MoP bearing surfaces were measured. In summary, this test scenario employed two new sets of samples with a sealed taper/trunnion interface tested for 0.5 million cycles. The two repetitions of the same test configuration in this test scenario were Samples 3 and 4. The electrochemical measurements of bearing surfaces (Samples 3 and 4) were compared to those of the long-term tests (Samples 1 and 2). The data comparison and surface analysis can potentially determine whether the bearing surface or taper/trunnion interface is the dominant potential source of the metallic tribocorrosion.

2.2.3 Effect of changing the serum solution on biotribocorrosion

Beadling et al. [12] combined an electrochemical cell with a hip simulator to investigate the corrosion rate of MoM bearings and determined that changing the serum could repeat OCP patterns. We also observed this phenomenon in the current study. The third series of tests were performed following the long-term test to improve our understanding of the relationship between the serum state and corrosion. More specifically, the test cell was rinsed three times with deionized water and continuously ran with the original serum solution. The fresh and used serum solutions were visually compared to investigate variations in their protein structure. Following this, the protein concentrations of the used lubricant from the soak and test stations were measured using a Pierce bicinchoninic acid assay kit [17] to trace the status of serum. Note that at each serum changing point, the soak and test stations were refreshed with the same fresh serum solution (i.e., the same batch).

In summary, Samples 1 and 2 were run for 1.5 million cycles to investigate the long-term biotribocorrosion of MoP THR. Sample 2 was tested for additional 0.5 million cycles with the used serum solution to determine the effect of the serum state on biotribocorrosion. Samples 3 and 4 with a sealed taper/trunnion interface were tested for 0.5 million cycles to examine the bearing surfaces' effects on biotribocorrosion.

2.3 Electrochemical measurements

All electrochemical measurements were conducted using a Princeton Applied Research P4000A electrochemical workstation (AMETEK, USA) at an acquisition rate of 1 Hz. The OCP was monitored during the entire test process. The OCP monitoring did not require the polarization of the test samples. Thus, the surfaces exhibited free-corrosion conditions, and a net current between the working and counter electrodes was absent. An OCP change represented a change in anodic and cathodic half-reactions rates, providing a semi-quantitative assessment of the WE passivation level.

Linear polarization resistance (LPR) was employed to determine the polarization resistance (R_P). The R_P and Stern and Geary equation [11] can be adopted to assess the I_{corr} of the system as Eq. (1):

$$I_{corr} = \frac{\beta_a \beta_c}{2.303 R_P (\beta_a + \beta_c)} \tag{1}$$

where β_a and β_c are Tafel constants. The LPR was measured every 10,000 s, with a measurement duration of 200 s, a scan range of ±20 mV from OCP with the scan rate of 0.33 mV/s, and β_a and β_c equal to 120 mV [11]. Since the polarization from OCP was of a low range, linear polarization was considered as a non-destructive technique.

2.4 Surface/chemical characterizations

The surface topography and appearance of each stem trunnion were examined using the laser scanning

confocal microscope (LSCM; MFT-500B, Rtec, USA) and scanning electron microscope (SEM; JSM-IT500, JEOL, Japan), respectively. The stem trunnion's three-dimensional surface roughness (R_Z) was measured using the LSCM (MFT-500B, Rtec, USA). Chemical analysis of the worn and unworn surfaces was performed using the energy-dispersive X-ray spectroscope (EDS; Ultim Extreme, UK). The chemical composition of the carbonaceous tribolayer was observed via the SEM and EDS, with more in-depth measurements performed using the confocal Raman spectroscope (LabRAM HR, HORIBA, Japan) with a record range of 1,000–2,000 cm^{-1}. The Raman spectra were fitted using the D and G lines of graphitic carbon [18] to distinguish the adhering proteins from carbonaceous tribofilms. All the surface/chemical measurements of the test specimens were performed before and after testing.

3 Results

3.1 Wear measurements

The gravimetric mass changes for the UHMWPE liner were recorded. The mean wear rate for 1.5 million cycles was 42.82±4.65 mg/10^6 cycles. The recorded wear rate was similar to a 28-mm head diameter UHMWPE liner [19, 20]. The details of the wear measurements of the articulating surfaces will be published in future work.

3.2 Biotribocorrosion of MoP THR during long-term walking gait cycles

Figure 2 presents the variations in the OCP patterns for Samples 1 and 2. In the static phase, the OCP remained at the relatively high levels of −60 and −39 mV for Samples 1 and 2, respectively, representing the presence of the oxide layer in the sample. During the static to the dynamic phase transition, the OCP exhibited an immediate decrease to −180 and −220 mV. The minimum values of −280 and −285 mV were subsequently reached around 0.125 million cycles. Following this, the OCP gradually increased to approximately −200 and −160 mV until the first serum was changed. The recovered OCP was lower than the initial OCP, indicating a change in the specimen corrosion state. The OCP variation trend repeated twice over the next two serum changes.

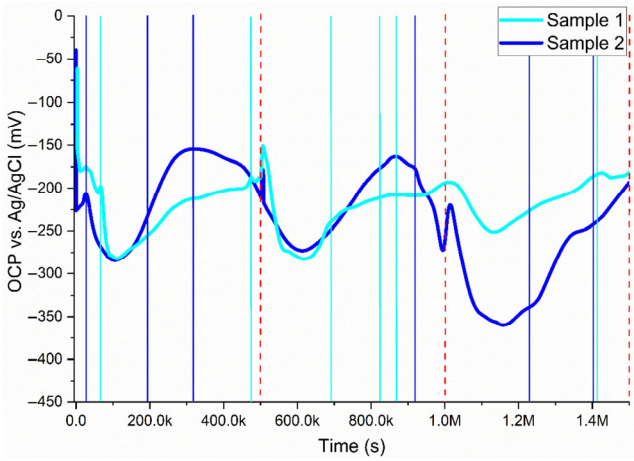

Fig. 2 Variations in the OCP for Samples 1 and 2. The vertical dashed lines represent the serum changing point, and the solid lines represent the machine stopping point.

Figure 3 depicts the I_{corr} for Samples 1 and 2, determined via the R_p and Stern Geary equation [11]. I_{corr} values exhibited an upward trend for both tests during the static to dynamic phase, and then kept relatively stable during the movement phase. The reduction in the amplitude of the first two OCP cycles in Sample 1 exceeded that of the last cycle, and I_{corr} variations exhibited a similar trend. For Sample 2, the third OCP cycle presented the largest decline, and I_{corr} also indicated the corrosion to be the strongest in the third cycle. Thus, I_{corr} variations agree with the OCP trends.

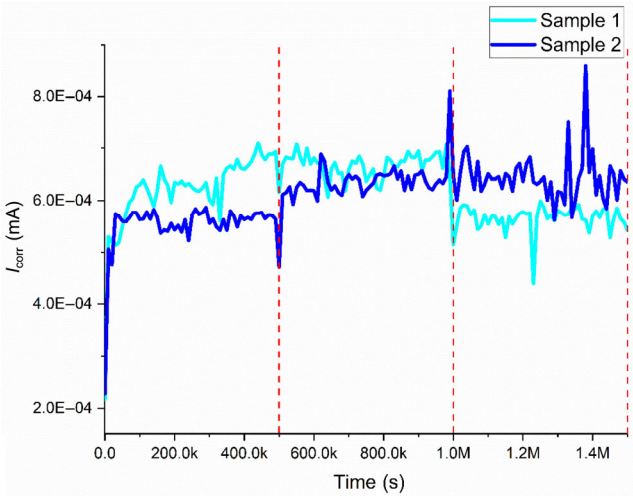

Fig. 3 Variations of I_{corr} corrosion currents for Samples 1 and 2.

3.3 Biotribocorrosion of the MoP THR bearing surface

Figure 4 demonstrates that Samples 3 and 4 presented a stable OCP trend. This indicates the limited bearing surface corrosion rate variation over the test period. Thus, the tribocorrosion from the taper/trunnion interface primarily affected the MoP THR corrosion rate variation. Moreover, the OCP values were greater, and the I_{corr} corrosion currents values were much smaller for Samples 3 and 4 than those for Samples 1 and 2 (Figs. 4 and 5). This implies the dominance of the metallic corrosion from the metal–metal contact (taper/trunnion interface) during long-term testing, which is in agreement with the clinical reports [3, 4] and previously published tests [8]. The electrochemical results of Samples 3 and 4 imply the taper/trunnion as the key active interface to be monitored in the electrochemical cell.

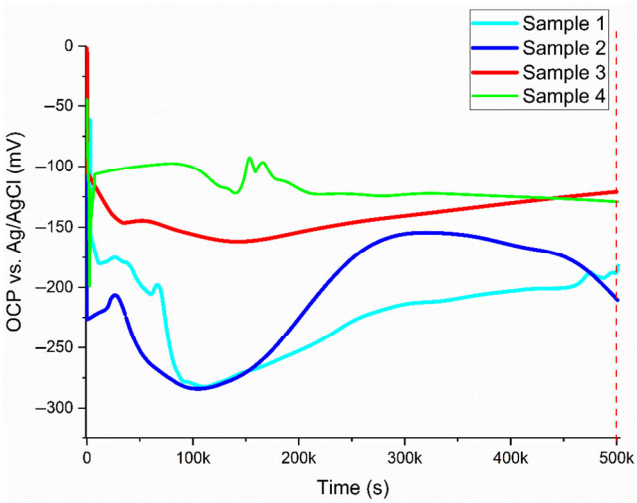

Fig. 4 Variations in the OCP for MoP THRs (Samples 1 and 2) and bearing surfaces (Samples 3 and 4) during 0.5 million cycles.

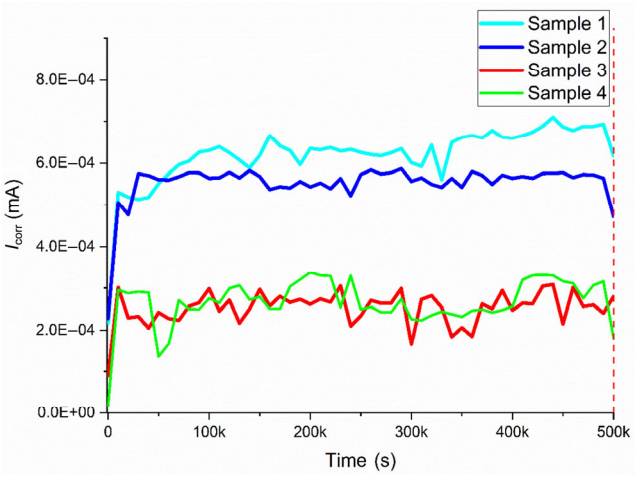

Fig. 5 Variations in the I_{corr} corrosion currents for MoP THRs (Samples 1 and 2) and bearing surfaces (Samples 3 and 4) during 0.5 million cycles.

3.4 Effect of changing the serum solution on biotribocorrosion

As detailed in Section 2.2, the third series of tests investigated the key influencing factor of the repeated OCP patterns. We measured the OCP variations in the test station filled with the used serum solution and kept the sample unchanged for 0.5 million cycles. The electrochemical measurements were compared with the previous OCP trends using the same serum solution. The light-yellow area (Stage I, Sample 2) in Fig. 6 was the last cyclic variation of Sample 2 in the long-term test, representing that the serum solution was changed with fresh serum, while the light-green area (Stage II, Sample 2) in Fig. 6 represents that the serum solution was unchanged. The OCP of Stage II displayed an initial reduction to −270 mV and quickly recovered to the final state of the previous OCP repetition (around −185 mV, Stage I). This state was maintained until the test terminated.

Visual comparisons reveal a difference in color between the fresh and used serum solutions of canary yellow and yellowish-white, respectively. Furthermore, according to the requirement of solution preparation from ISO 14242-1, the fresh serum passed the 2-μm filter while the used one did not. The previous research

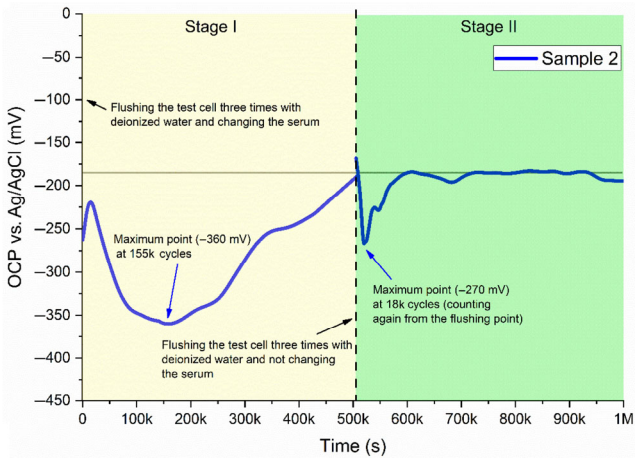

Fig. 6 Variation in OCP for a change (Stage I, Sample 2) and no change (Stage II, Sample 2) in the serum solution.

reported that the proteins within the serum solution greatly impact corrosion [21]. The current study results revealed that the serum change induces the repetition of OCP trends in the MoP hip prosthesis. Thus, the protein variations within the serum solution altered the corrosion rate. Table 1 reports the protein concentrations in the used serum solution of the soak and test stations throughout the long-term test to investigate the relationship between the protein concentration and wear-corrosion. The protein concentrations of the soak station exceeded those of the test stations. The soak station was only subjected to the axial force without the applied motion compared with the test station. Thus, the protein concentration declined due to wearing.

Table 1 Protein concentrations of soak and test stations during the test period.

Station/No. of cycles	Protein concentration (g/L)
Soak/500k	38.16±0.87
Soak/1,000k (first serum change)	38.72±0.58
Soak/1,500k (second serum change)	37.27±0.09
Sample 1/500k	34.95±0.85
Sample 1/1,000k (first serum change)	34.94±0.16
Sample 1/1,500k (second serum change)	34.55±0.30
Sample 2/500k	34.94±0.16
Sample 2/1,000k (first serum change)	34.28±0.96
Sample 2/1,500k (second serum change)	28.35±0.41

3.5 Surface topography

Figure 7 presents the surface topographies of the femoral head bearing surface (CoCrMo) obtained using the SEM. No significant corrosion signs were observed at the bearing surface of the post-test femoral head compared with the pre-test case. However, scratches appeared at the post-test bearing surface, mainly attributed to mechanical sliding and wear.

Following the test, the stem trunnion was disassembled from the femoral head based on ISO 7206-10. The pre- and post-test taper trunnions were examined by the LSCM and SEM. The pre-test trunnion surface exhibited clear machining marks. The wear debris and the corrosive particles were mounded beside the worn area of the post-test trunnion, which increased R_Z from 12.14±0.29 to 14.96±1.48 μm (Fig. 8). This agrees with the retrieved implant results of Cadel et al. [5]. The deposited layer was also observed in the SEM images (Fig. 9). The EDS observations further revealed that the layers on the worn surface were

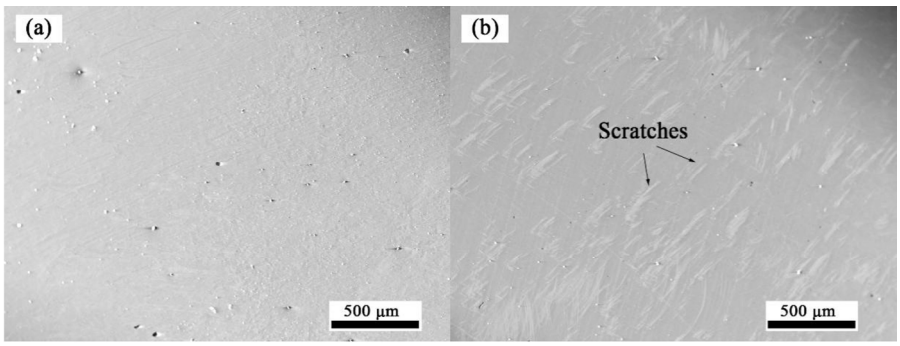

Fig. 7 SEM images at 50× magnification of the femoral head bearing surface: (a) before and (b) after the test.

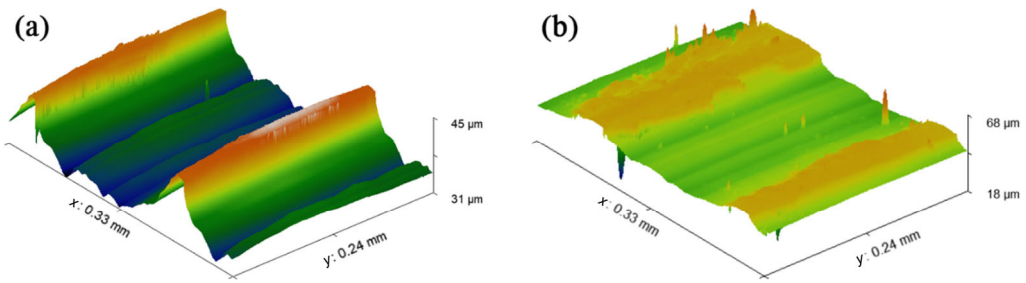

Fig. 8 LSCM images at 50× magnification of the stem trunnion: (a) before (R_Z = 12.14±0.29 μm) and (b) after (R_Z = 14.96±1.48 μm) the test.

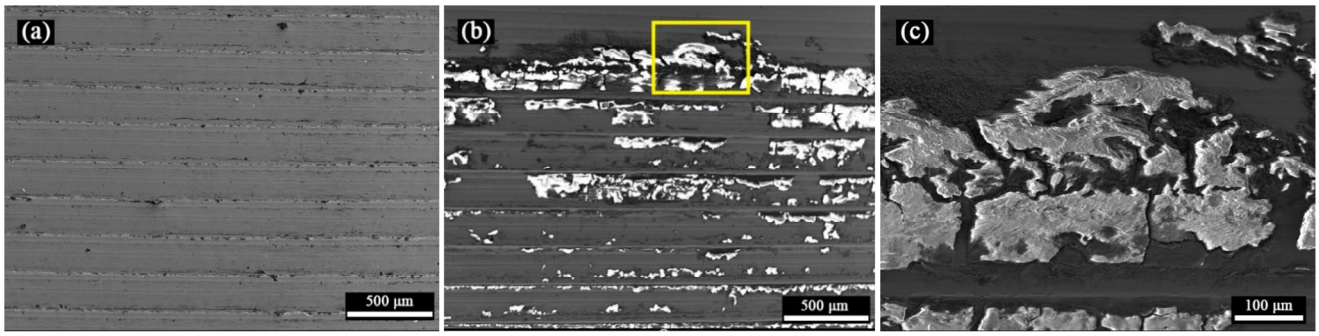

Fig. 9 SEM images at 50× the magnification of the stem trunnion: (a) before and (b) after the test. (c) Magnified view (200×) of the worn area indicated by the yellow box in (b).

carbon-rich and contained oxygen and femoral head constituents (e.g., cobalt, chromium, and molybdenum) (Fig. 10). The EDS analysis also indicates that the appearance of the carbon-rich deposited layer was attributed to the synergies between the fretting wear and corrosion. The Raman spectroscopy confirmed that the deposited layer was the nanocrystalline graphite and amorphous sp^2 carbon tribological layer [18]. The D- and G-peaks were present at around 1,404.0 and 1,575.2 cm^{-1}, respectively (Fig. 11).

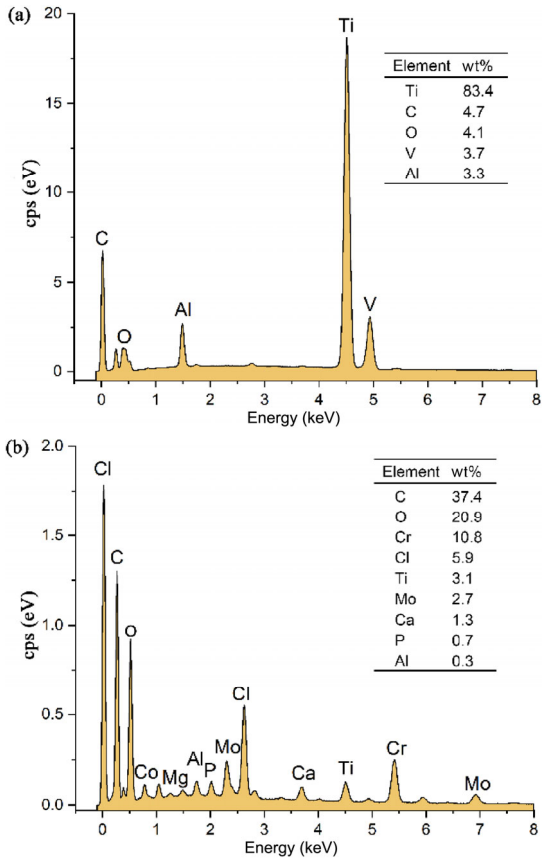

Fig. 10 EDS analysis of (a) unworn and (b) worn surfaces.

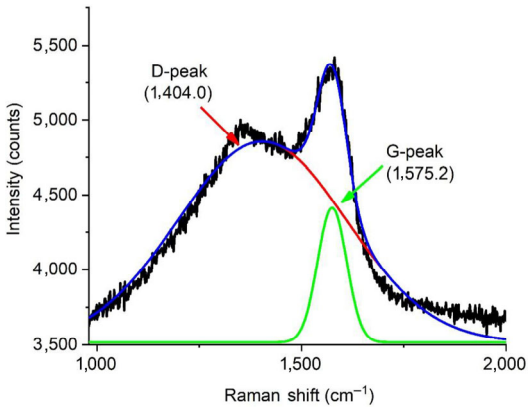

Fig. 11 Raman spectrum of the worn surface at the stem trunnion.

4 Discussion

4.1 Evolution of the corrosion behavior in long-term walking gait

For Samples 3 and 4, the OCP values were larger, and the corrosion currents were much smaller than those of Samples 1 and 2, while the OCP trend of the former was more stable. This indicates that the tribocorrosion from the taper/trunnion interface was the principal factor influencing the corrosion rate variations of MoP THR. In addition, the surface characterizations identified only mechanical damage on the post-test bearing surface, with no significant signs of corrosion. Consequently, the dominance of biotribocorrosion at the taper/trunnion interface of MoP THR was confirmed. Such findings were consistent with the retrieved clinical studies [3, 4, 22].

Under the long-term walking gait cycles, three clear periodicities in the OCP trends were observed for Samples 1 and 2. This observation may be attributed to three factors: 1) the termination of the

machine, 2) the flushing of the test cells by deionized water, and 3) the change of serum solution, all of which could damage the passive film or break the corrosion status balance. The OCP repetition caused by the "machine stop" was firstly excluded, because its effect on the OCP was insignificant, as shown in Fig. 2. Therefore, following the long-term test, Sample 2 was continuously tested with the same serum solution to determine which subsequent factors were the underlying cause. Then the electrochemical measurements of Sample 2 with fresh (Stage I) and used (Stage II) serum solutions were compared. The corrosion evolution trend from Fig. 6 indicates that although flushing affected the corrosion variations, the serum change influence was dominant. The used serum was able to protect the test samples from corrosion.

Talha et al. [21] determined that proteins significantly influenced corrosion as they could be adsorbed on the metal surface, creating a barrier between the lubricant and metal surface. Wang et al. [23] reported that proteins that were less stable and close to their isoelectric point, or those with a larger size and unfolding rate, could be readily adsorbed on the metal surface. The visual observations in this study demonstrated a color change in the used serum solution. Furthermore, unlike the fresh serum solution, the used serum could not pass the 2-μm filter, indicating protein precipitation and aggregation. By integrating our results with those of the literature, it was assumed that the precipitated and aggregated proteins with a larger molecule size were more likely to be adsorbed on the metal surface, resulting in the formation of the adsorbed protein layer. This adsorbed protein layer inhibited corrosion by isolating the metal surface from the serum solution, while the fresh serum did not. Thus, the adsorbed protein layer could not be regenerated with the application of the fresh serum. Furthermore, the adhesion force between the adsorbed protein layer and the metal surface was weak. Hence the adsorbed protein layer could be easily rinsed out from the surface via deionized water. This assumption could explain the corrosion evolution trend between the fresh and used serum solution in Fig. 6. The adsorbed protein layer was damaged after flushing, consequently increasing the corrosion corresponding to Stage II of Sample 2. The precipitated and aggregated proteins within the used serum solution rebuilt the adsorbed layer, implying that the corrosion quickly recovered to the final state of the last OCP repetition (Stage I, Sample 2) and subsequently maintained stable at this state. The adsorbed protein layer of the fresh serum solution was permanently damaged, preventing its rapid regeneration. This was the primary reason for the repeated corrosion trends.

At each cyclic variation of the corrosion, the initial corrosion increase indicated the mechanical damage of the material oxide layer after applying the force and motion. This is a common phenomenon of MoM or MoP bearings for both hip simulators and pin/ball-on-disc tribometers [8, 11, 16, 24]. The depassivation of the taper/trunnion interface was dominant until the turning point (at approximately 0.125 million cycles). This was linked to the fretting wear and corrosion synergism, leading to the passive film breakdown and the material degradation. Repassivation subsequently became the dominant factor. This may be attributed to the faster recovery rate of the passive film than the rates of alloy dissolution and mechanical damage. Following the gentle decline in corrosion, a relatively steady-state stage was observed. This stage, which indicates a balance between the depassivation and repassivation, was not observed in the second and third cycles of the OCP patterns in Sample 2. Such a phenomenon reveals a change in the serum or the termination of the test before the degradation and passivation rates could achieve equilibrium.

4.2 Formation and function of the tribolayer on the taper/trunnion interface

The protein concentration of the soak and test stations indicates that the proteins within the serum solution reacted with the test samples under the wear condition. The tribochemical reaction layer (termed tribolayer) observed on the taper/trunnion interface's worn surface may have been one of the reaction products. The Raman spectral signals were similar to tribolayer signals with hard-on-hard bearing surfaces (carbonaceous layer) [18], confirming the appearance of carbonaceous tribolayers at the taper/trunnion interfaces. The tribolayer is commonly assumed to be made of denatured proteins [25–27], with graphitic

carbon as the principal chemical component [18]. The tribolayer may be formed via a two-step process under continuous sliding: 1) The proteins are adsorbed to the metal surfaces serving as solid lubricants [14] and 2) this adsorption layer is converted to the tribological film (tribolayer) under the wear condition [28, 29]. The carbon-rich tribolayer firmly adheres to MoM bearing surfaces [27, 30] with lubricating and isolating effects that can lower the prostheses' wear rate and corrosion rate [8, 30–33]. Similar tribolayers were identified on the taper/trunnion interface compared with MoM bearing surfaces [18]; thus, it was assumed that the tribolayer formation and function on the taper/trunnion interface were equal to those on MoM bearing surfaces. As a result, the tribolayer formed on the worn surface could contribute to the noble shifts in potential and consequently inhibit corrosion.

4.3 Hypothesis of the tribocorrosion mechanism

Based on the current study and previous literature, it is possible to infer the tribocorrosion mechanism at the taper/trunnion interface. After the test started, the bulk material oxidation layer was damaged by either mechanical wear or chemical dissolution. Chemical and mechanical reactions subsequently occurred between the exposed bare metallic surface and the corrosive medium, resulting in a sudden increase in corrosion. During the tests, two passivation films formed on the surface of the taper/trunnion interface, namely, an adsorbed protein layer from the precipitated and aggregated proteins and the tribolayer from the denatured proteins and wear debris. The reduction in corrosion was likely the result of the formation of the two types of layers, indicating the corrosion inhibitory ability of both layers. The adhesion force of the adsorbed protein layer was weaker than that of the tribolayer, while the opposite was true for the corrosion resistance. This explains why deionized water rinsed the adsorbed protein layer at the serum changing point, while the tribolayer was preserved on the worn surface after the test. Moreover, the adsorbed layer damage immensely influenced the system's corrosion. The precipitated and aggregated proteins that made the adsorbed protein layer possibly started forming at approximately 0.125 million cycles, marking the turning point of corrosion.

4.4 Limitations

This study did not measure the femoral head and stem trunnion volume losses. Furthermore, according to ISO 14242-1 requirement, the full hip wear test should complete 5 million cycles. Since this study was a preliminary test, it ran for just 1.5 million cycles. However, the test duration used here was still the longest compared with the published literature. Future work will focus on the complete 5-million-cycle test and the effect of the test duration on the tribocorrosion behavior. An additional limitation is the lack of an in-depth investigation of the tribolayer evolution mechanism. The transmission electron microscopy (TEM) can be employed to comprehensively evaluate the tribolayer structure and composition by analyzing its underlying surfaces. Nano test techniques, such as the atomic force microscopy (AFM) and nanoindentation, can also be introduced to assess the mechanical properties of the tribolayer to better understand its role in the tribocorrosion process.

5 Summary

The current study reports the first MoP THR *in-situ* electrochemical measurements under the long-term walking gait. These live *in-situ* measurements provide valuable insight into the biotribocorrosion mechanism. Key observations of this work are summarized as follows:

1) The modular taper/trunnion junction was the main cause of MoP THR biotribocorrosion.

2) Changing the serum solution was the main factor for the repetition of the corrosion variation at the taper/trunnion junction in the long-term walking gait cycles. The typical serum changing point 0.5 million cycles) was considered long enough for the degradation and passivation rates to achieve the dynamic equilibrium.

3) Each OCP repetition exhibited a similar corrosion rate trend. The corrosion was immediately enhanced after applying motion and force, reaching a maximum at approximately 0.125 million cycles, followed by a gradual reduction.

4) The adsorbed protein layer formation and disruption markedly affected the corrosion evolution

in MoP THR. This protein adsorption layer principally caused the long-term passivation.

5) A carbon-rich proteinaceous layer was observed on the worn surface of the stem trunnion. This layer was similar to the tribolayer observed on the MoM bearing surfaces.

Acknowledgements

This work was supported by the National Natural Science Foundation of China (52035012), the Science and Technology Planning Project of Sichuan Province (2020YJ0032), and the 111 Project (B20008).

References

[1] Zhang X G, Zhang Y L, Jin Z M. A review of the bio-tribology of medical devices. *Friction* **10**(1): 4–30 (2022)

[2] Cook R B, Bolland B J R F, Wharton J A, Tilley S, Latham J M, Wood R J K. Pseudotumour formation due to tribocorrosion at the taper interface of large diameter metal on polymer modular total hip replacements. *J Arthroplasty* **28**(8): 1430–1436 (2013)

[3] Persson A, Eisler T, Bodén H, Krupic F, Sköldenberg O, Muren O. Revision for symptomatic pseudotumor after primary metal-on-polyethylene total hip arthroplasty with a standard femoral stem. *J Bone Joint Surg Am* **100**(11): 942–949 (2018)

[4] Hussey D K, McGrory B J. Ten-year cross-sectional study of mechanically assisted crevice corrosion in 1,352 consecutive patients with metal-on-polyethylene total hip arthroplasty. *J Arthroplasty* **32**(8): 2546–2551 (2017)

[5] Cadel E S, Topoleski L D T, Vesnovsky O, Anderson C R, Hopper Jr R H, Engh Jr C A, di Prima M A. A comparison of metal/metal and ceramic/metal taper-trunnion modular connections in explanted total hip replacements. *J Biomed Mater Res B Appl Biomater* **110**(1): 135–143 (2022)

[6] Siljander M P, Baker E A, Baker K C, Salisbury M R, Thor C C, Verner J J. Fretting and corrosion damage in retrieved metal-on-polyethylene modular total hip arthroplasty systems: What is the importance of femoral head size? *J Arthroplasty* **33**(3): 931–938 (2018)

[7] Royhman D, Patel M, Runa M J, Jacobs J J, Hallab N J, Wimmer M A, Mathew M T. Fretting-corrosion in hip implant modular junctions: New experimental set-up and initial outcome. *Tribol Int* **91**: 235–245 (2015)

[8] Hesketh J, Hu X M, Dowson D, Neville A. Tribocorrosion reactions between metal-on-metal and metal-on-polymer surfaces for total hip replacement. *Proc Inst Mech Eng Part J J Eng Tribol* **226**(6): 564–574 (2012)

[9] Pu J, Wu D S, Zhang Y L, Zhang X G, Jin Z M. An experimental study on the fretting corrosion behaviours of three material pairs at modular interfaces for hip joint implants. *Lubricants* **9**(2): 12 (2021)

[10] Bhalekar R M, Smith S L, Joyce T J. Hip simulator testing of the taper-trunnion junction and bearing surfaces of contemporary metal-on-cross-linked-polyethylene hip prostheses. *J Biomed Mater Res Part B Appl Biomater* **108**(1): 156–166 (2020)

[11] Hesketh J, Hu X M, Yan Y, Dowson D, Neville A. Biotribocorrosion: Some electrochemical observations from an instrumented hip joint simulator. *Tribol Int* **59**: 332–338 (2013)

[12] Beadling A R, Bryant MG, Dowson D, Neville A. The effect of microseparation on corrosion rates of metal-on-metal total hip replacements. In: Proceedings of the NACE International Corrosion Conference, Dallas, USA, 2015: NACE-2015-5599.

[13] Beadling A R, Bryant M G, Dowson D, Neville A. Adverse loading effects on tribocorrosive degradation of 28 mm metal-on-metal hip replacement bearings. *Proc Inst Mech Eng Part J J Eng Tribol* **235**(12): 2664–2674 (2021)

[14] Yan Y, Neville A, Dowson D, Williams S, Fisher J. Electrochemical instrumentation of a hip simulator: A new tool for assessing the role of corrosion in metal-on-metal hip joints. *Proc Inst Mech Eng H* **224**(11): 1267–1273 (2010)

[15] Weber P, Schröder C, Schwiesau J, Utzschneider S, Steinbrück A, Pietschmann M F, Jansson V, Müller P E. Increase in the tibial slope reduces wear after medial unicompartmental fixed-bearing arthroplasty of the knee. *Biomed Res Int* **2015**: 736826 (2015)

[16] Hesketh J, Meng Q G, Dowson D, Neville A. Biotribocorrosion of metal-on-metal hip replacements: How surface degradation can influence metal ion formation. *Tribol Int* **65**: 128–137 (2013)

[17] Brandt J M, Charron K D, Zhao L, MacDonald S J, Medley J B. Lubricant biochemistry affects polyethylene wear in knee simulator testing. *Biotribology* **27**: 100185 (2021)

[18] Liao Y, Pourzal R, Wimmer M A, Jacobs J J, Fischer A, Marks L D. Graphitic tribological layers in metal-on-metal hip replacements. *Science* **334**(6063): 1687–1690 (2011)

[19] Smith S L, Unsworth A. A comparison between gravimetric and volumetric techniques of wear measurement of UHMWPE acetabular cups against zirconia and cobalt-chromium-molybdenum femoral heads in a hip simulator. *Proc Inst Mech Eng Part H J Eng Med* **213**(6): 475–483 (1999)

[20] Affatato S, Zavalloni M, Taddei P, di Foggia M, Fagnano C, Viceconti M. Comparative study on the wear behaviour of different conventional and cross-linked polyethylenes for total hip replacement. *Tribol Int* **41**(8): 813–822 (2008)

[21] Talha M, Ma Y C, Kumar P, Lin Y H, Singh A. Role of protein adsorption in the bio corrosion of metallic implants—A review. *Colloids Surf B Biointerfaces* **176**: 494–506 (2019)

[22] Hall D J, Pourzal R, Jacobs J J. What surgeons need to know about adverse local tissue reaction in total hip arthroplasty. *J Arthroplasty* **35**(6): S55–S59 (2020)

[23] Wang K F, Zhou C C, Hong Y L, Zhang X D. A review of protein adsorption on bioceramics. *Interface Focus* **2**(3): 259–277 (2012)

[24] Yan Y, Neville A, Dowson D, Williams S, Fisher J. The influence of swing phase load on the electrochemical response, friction, and ion release of metal-on-metal hip prostheses in a friction simulator. *Proc Inst Mech Eng Part J J Eng Tribol* **223**(3): 303–309 (2009)

[25] Maskiewicz V K, Williams P A, Prates S J, Bowsher J G, Clarke I C. Characterization of protein degradation in serum-based lubricants during simulation wear testing of metal-on-metal hip prostheses. *J Biomed Mater Res Part B Appl Biomater* **94B**(2): 429–440 (2010)

[26] Chan F W, Bobyn J D, Medley J B, Krygier J J, Yue S, Tanzer M. Engineering issues and wear performance of metal on metal hip implants. *Clin Orthop Relat Res* **333**: 96–107 (1996)

[27] Wimmer M A, Sprecher C, Hauert R, Täger G, Fischer A. Tribochemical reaction on metal-on-metal hip joint bearings: A comparison between *in-vitro* and *in-vivo* results. *Wear* **255**(7–12): 1007–1014 (2003)

[28] Wimmer M A, Fischer A, Büscher R, Pourzal R, Sprecher C, Hauert R, Jacobs J J. Wear mechanisms in metal-on-metal bearings: The importance of tribochemical reaction layers. *J Orthop Res* **28**(4): 436–443 (2010)

[29] Pourzal R, Theissmann R, Williams S, Gleising B, Fisher J, Fischer A. Subsurface changes of a MoM hip implant below different contact zones. *J Mech Behav Biomed Mater* **2**(2): 186–191 (2009)

[30] Hesketh J, Ward M, Dowson D, Neville A. The composition of tribofilms produced on metal-on-metal hip bearings. *Biomaterials* **35**(7): 2113–2119 (2014)

[31] Pourzal R, Martin E J, Vajpayee S, Liao Y, Wimmer M A, Shull K R. Investigation of the role of tribofilms in self-mating CoCrMo systems utilizing a quartz crystal microtribometer. *Tribol Int* **72**: 161–171 (2014)

[32] Taufiqurrakhman M, Neville A, Bryant M G. The effect of protein structure and concentration on tribocorrosion and film formation on CoCrMo alloys. *J Bio Tribo Corros* **7**(4): 147 (2021)

[33] Wang Z W, Yan Y, Su Y J, Qiao L J. Effect of proteins on the surface microstructure evolution of a CoCrMo alloy in bio-tribocorrosion processes. *Colloids Surf B Biointerfaces* **145**: 176–184 (2016)

Shu YANG. He received his M.S. degree in mechanical engineering in 2013 from Imperial College London, London. Currently, he is a Ph.D. student in Southwest Jiaotong University, China. His research interests include wear and biotribocorrosion of hip prosthesis.

Jian PU. He received his M.S. degree in mechanical engineering in 2020 from Southwest Jiaotong University, China. Currently, he is a Ph.D. student in the Southwest Jiaotong University, China. His research interests include fretting wear and fretting corrosion of hip prosthesis.

Xiaogang ZHANG. He received his Ph.D. degree in mechanical engineering in 2017 from The University of New South Wales, Australia. He joined the Tribology Research Institute at Southwest Jiaotong University, China, as an assistant researcher in 2018. His current research interests focus on the musculoskeletal biomechanics and biotribology.

Yali ZHANG. She received her Ph.D. degree in mechanical engineering in 2013 from Xi'an Jiaotong University, China. She joined the School of Mechanical Engineering at Southwest Jiaotong University, China, as a lecturer in 2015. Her current research interests focus on the biotribology of artificial joints.

Zhongmin JIN. He received his Ph.D. degree in mechanical engineering in 1984 from University of Leeds, UK. He joined the School of Mechanical Engineering at Southwest Jiaotong University (SWJTU), China, from 2015. His current position is a professor and the dean of the SWJTU–Leeds Joint School. His current research interests include biotribology, biomechanics and medical devices, artificial joint design and manufacturing, and tissue engineering.